Archives of Mechanics • Archiwum Mechaniki Stosowanej • 26, 2, pp. 181–185, Warszawa 1974

Non-equilibrium ionized radiating boundary layer flow over a blunt body

YU. P. LUNKIN, S. B. KOLESHKO and I. Z. FINEBERG (LENINGRAD)

THE PRESENT paper is devoted to the consideration of steady axisymmetric flow of nonequilibrium ionized monoatomic radiating gas (argon) on a spherically blunted body. Calculation is performed of transport coefficients as the functions of thermodynamic parameters. Profiles of temperature and degree of ionization are obtained.

Praca poświęcona jest zagadnieniom ustalonego przepływu niezrównoważonego, zjonizowanego gazu (argonu) wokół sferycznie stępionego ciała. Wyznaczono współczynniki transportu jako funkcje parametrów termodynamicznych. Otrzymano wykresy temperatury oraz współczynnika jonizacji.

Работа посвящена проблемам установившегося течения неравновесного, ионизованного газа (аргона) вокруг сферически затупленного тела. Определены кинетические коэффициенты как функции термодинамических параметров. Получены диаграммы температуры и коэффициента ионизации.

1. Introduction

IONIZATION and radiation have a decisive effect on gas energy balance in the boundary layer during hypersonic flight. These processes may significantly influence each other, since the variation of degree of ionization may be caused not only by the particle collisions but by photoionization and photorecombination. On the other hand, the radiation field depends on the correlation between the concentration in the gas mixture of ion, electron and neutral particles. Coupling of the processes mentioned above was considered in paper [1] for nonviscid gas. Boundary layer calculation is accompanied by additional difficulties connected with the calculation of transport coefficients which have certain peculiarities in high-temperature ionized gas.

1. Governing set of equations

Using the monoatomic quasi-neutral gas ionization and radiation model proposed in the paper [2], we obtain the following equations of the transparant boundary layer:

$$\frac{\partial}{\partial}(r^j \varrho u)+\frac{\partial}{\partial y}(r^j \varrho v) = 0, \tag{1.1}$$

$$\varrho u\frac{\partial u}{\partial x}+\varrho v\frac{\partial u}{\partial y} = -\frac{dp}{dx}+\frac{\partial}{\partial y}\left(\mu\frac{\partial u}{\partial y}\right), \tag{1.2}$$

$$\varrho u\frac{\partial h}{\partial x}+\varrho v\frac{\partial h}{\partial y} = \frac{\partial}{\partial y}\left(\lambda\frac{\partial T}{\partial y}\right)+\frac{\partial}{\partial y}\left(\varrho D_A\frac{\partial h}{\partial \alpha}\frac{\partial \alpha}{\partial y}\right)+u\frac{dp}{dx}+\mu\left(\frac{\partial u}{\partial y}\right)^2-\varrho(\dot{h})_R, \tag{1.3}$$

$$\varrho u \frac{\partial \alpha}{\partial x} + \varrho v \frac{\partial \alpha}{\partial y} = \frac{\partial}{\partial y}\left(\varrho D_A \frac{\partial \alpha}{\partial y}\right) + \frac{\varrho \alpha}{\tau}\left(\frac{1-\alpha}{1-\alpha_E}\alpha_E^2 - \alpha^2\right) - \varrho(\dot{\alpha})_R, \tag{1.4}$$

$$p = \varrho(1+\alpha)kT/m_a. \tag{1.5}$$

Here, in addition to the usual boundary layer theory notations, the following notations are adopted: α — degree of ionization; h — specific enthalpy of mixture; μ, λ, D_A — viscosity, heat-conductivity and ambipolar diffusion coefficients; τ — characteristic time of non-equilibrium processes of collisional ionization and recombination; $(\dot{h})_R$, $(\dot{\alpha})_R$ — rate of enthalpy and degree of ionization variation due to photorecombination. Values $(\dot{h})_R$ and $(\dot{\alpha})_R$ are determined by the relations obtained in paper [2].

After Dorodnitsin-Lees transformation [3] of the equations (1.1)–(1.4), only the following non-dimensional complexes will contain the transport coefficients: $l = \dfrac{p_0 \mu \varrho}{p(\mu\varrho)_{eo}}$ — Chapmen-Rubesin parameter; $\Pr = \mu \dfrac{\partial h}{\partial T} \Big/ \lambda$ — Prandtl number; $\mathrm{Sc} = \mu/\varrho D_A$ — Schmidt number; $\mathrm{Le} = \Pr/\mathrm{Sc}$ — Luise number; subscript "eo" concerns the parameters on the outer edge on the axis of symmetry; p_0 — stagnation point pressure.

The distribution of parameters on the outer edge of the boundary layer has to be taken from the solution of the nonviscid blunt body problem with the same relaxation processes taken into account. Body surface is usually considered as noncatalytic or absolutely catalytic. These are the boundary conditions on the body surface. In the case of transparent boundary layer considered, there is, in the special boundary condition, no need for the radiation field because radiative terms are expressed through local thermodynamic parameters.

2. Calculation of transport coefficients

As a rule, Sonin's polynomes expansion of the partition function is used for calculation of the transport coefficient [4]. When dissociation is taken into account, the one-term approximation for μ, D, and the two-term approximation for λ are quite acceptable. However, these approximations are insufficient for ionized gases [5]. The convergence rate for argon was investigated in the papers [5, 6]. It was shown that the two-term approximation is sufficient for μ and the four-term approximation — for λ and D. Final results were obtained only for the case of equilibrium ionization.

Let us use the method proposed in the paper [6] for calculation of transport coefficient in the case of non-equilibrium ionized argon. We shall disregard the terms of order $(m_e/m_a)^{1/2}$, and smaller terms in the determinant elements in using the corresponding expressions.

The ambipolar diffusion coefficient is determined by the expression:

$$D_A = 2D_{ia}\left[1 - \frac{m_e}{m_a}\frac{D_{ie}}{D_{ia}}\left(1 - \frac{D_{ea}}{D_{ei}}\right)\right], \tag{2.1}$$

where D_{ie}, D_{ia}, D_{ea}, D_{ei} — generalized diffusion coefficients of the corresponding components. For the one-term approximation

$$D_{ia} \approx D_{ai} \approx D_{ia}^{*}, \quad D_{ea} \approx D_{ei}, \tag{2.2}$$

where D^*_{ia} — binar diffusion coefficient. We shall suppose [4] that relations (2.2) are valid for higher approximations. Then $D_A \approx 2[D^*_{ia}]_1$, where $[D^*_{ia}]_1$ — one-term approximation of binar ion-atom diffusion coefficient [4]. Finally, the problem is to determine the interaction potentials which are necessary for calculation of the gas kinetic $\sigma^{(l)}_{ij}$ and average cross-sections S^{ls}_{ij}.

There are three types of interaction in collisions of plasma particles: a) between charged particles, b) between charged and neutral particles, c) between neutral particles. Let us consider every type of interaction.

a. In calculation $\sigma^{(l)}_{ij}$ for charged particles it was supposed [6] that for large deviation angles the interaction potential is equal to Coulomb's and for small deviation angles — to screened Coulomb's potential $\Phi = \frac{z_i z_j e^2}{r} \exp\left(-\frac{r}{d}\right)$, where $z = -1$ for electron and $z = 1$ for ion, and $d = (kT/8\pi n_e e^2)^{1/2}$ — the Debye length, obtained by taking into account the screening from electrons and ions.

b. Results of [6] were used for $\sigma^{(1)}$ in calculation of the gas kinetic cross-sections for electron-atom collisions and it was supposed that $\sigma^{(2)} = \sigma^{(3)} = \sigma^{(4)} = \sigma^{(1)}$; in calculation of the ion-atom cross-section for even l the relation $\sigma^{(l)}_{ia} - \sigma^{(l)}_{aa}$ was used, and for odd l the approximation $\sigma^{(l)} = (25.61 - 1.196 \ln g)^2$, where relative velocity g is expressed in cm/sec and $\sigma^{(l)}$ – in Å.

c. The experimental potential expression [7] was used for atom-atom collisions

$$\Phi = \Phi_0 \exp\left(-\frac{r}{\mathscr{D}}\right), \text{ where } \Phi_0 = 32\,300\,\text{eV}, \mathscr{D} = 0.224\,\text{Å}.$$

Calculation showed that, by contrast with the case of equilibrium, transport coefficients of ionized gases in the case considered are functions of three independent variables: temperature, pressure (through the Debye length) and degree of ionization. The main results are presented in Figs. 1–3.

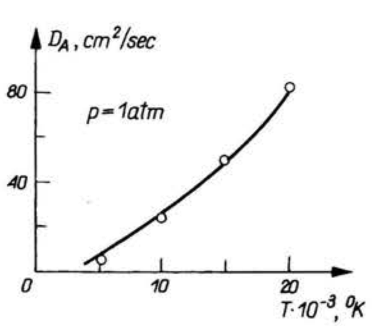

FIG. 1. Behaviour of the ambipolar diffusion coefficient.

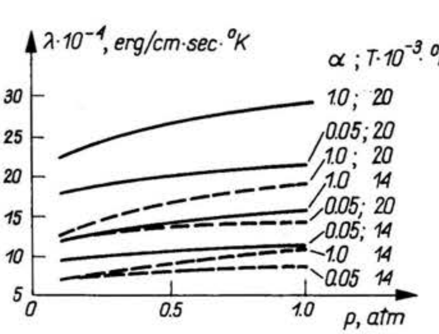

FIG. 2. Behaviour of the thermoconductivity coefficient.
Unbroken and dotted lines concern four-term and two-term approximations, respectively.

Function $D_A = CT^{1.66}$ is shown in Fig. 1 by dots. The viscosity coefficient depends weakly on pressure, enabling us to consider it as a function only of T and α.

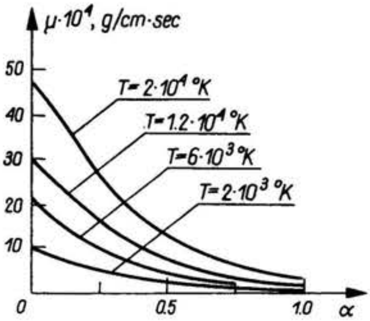

FIG 3. Behaviour of the viscosity coefficient.

Note that the range of parameters variation where transport coefficients are calculated is bounded by the conditions which enable the use of a truncated Coulomb potential for charged particles. The principal difficulties appear with relatively low temperature and high pressure.

3. Calculation of the boundary layer flow

The set of Eqs. (1.1)–(1.5) was solved for a spherically blunted body with bluntness radius R. By way of example, profiles of stagnation point gas dynamic parameters are presented for the case $R = 40\text{cm}$, $M_\infty = 28.9$, $p_\infty = 10^{-4}\text{atm}$, $T_\infty = 300°\text{K}$. The body surface was accepted as being absolutely catalytic as regards surface ionization, $T_w = 2000°\text{K}$. Solution was obtained by means of the marching method with application of iterative technique. For comparison, the flow with non-equilibrium ionization but without radiation in the boundary layer or in the outer region was calculated. Some results are presented in Figs. 4–7; unbroken and dotted lines represent radiating and non-radiating

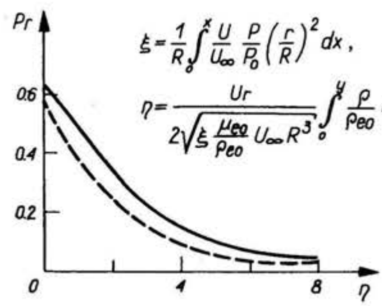

$$\xi = \frac{1}{R}\int_0^x \frac{U}{U_\infty}\frac{P}{P_0}\left(\frac{r}{R}\right)^2 dx,$$

$$\eta = \frac{Ur}{2\sqrt{\xi \frac{\mu_{eo}}{\rho_{eo}} U_\infty R^3}}\int_0^y \frac{\rho}{\rho_{eo}} dy$$

FIG. 4. Behaviour of the Prandtl number.

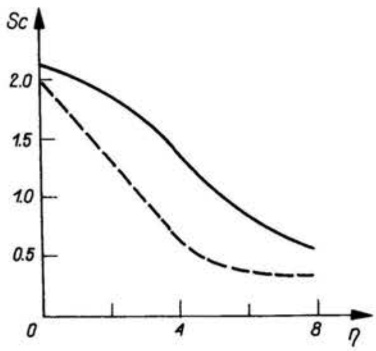

FIG. 5. Behaviour of the Schmidt number.

flow, respectively. As was to be expected, heat conductivity increases significantly and the Prandtl number significantly decreases in ionized gas due to the presence of electrons. Distributions of Pr, Sc across the boundary layer are shown in Figs. 4–5.

Temperature distribution across the boundary layer is shown in Fig. 6. Note first the significant increase of boundary layer thickness and temperature reduction as compared with the case $Pr = Sc = 1$. Analogous conclusions may be drawn as regards the degree of ionization profiles (Fig. 7).

Under the conditions considered, radiation markedly influences the degree of ionization distribution and comparatively weakly — the temperature distribution. Radiation (photorecombination) results in the reduction of electron concentration and increases

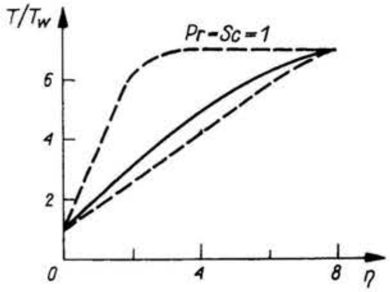

FIG. 6. Behaviour of the temperature.

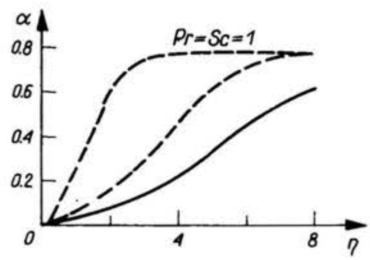

FIG. 7. Behaviour of the ionization degree.

the gas temperature. The explanation of the latter effect is as follows: when α markedly decreases, the heat conductivity coefficient also decreases and the Prandtl number increases, finally resulting in a temperature increase. This example shows that accurate definition of transport coefficients is of great importance in the calculation of non-equilibrium ionized radiating gas flow in the boundary layer.

References

1. М. Д. КРЕМЕНЕЦКИЙ, Н. В. ЛЕОНТЬЕВА, Ю. П. ЛУНЬКИН, ПМТФ, 4, 1971.
M. D. KREMENETSKII, N. W. LEONT'EVA, YU. P. LUNKIN, PMTF, 4, 1971.
2. J. H. CLARKE, C. FERRARI, Phys. Fluids, **8**, 12, 2121, 1965.
3. Л. Г. Лойцянский, *Механика жидкости и газа* [L. G. Loutsyanskii, Mechanics of fluids and gases], "Наука", 1970.
4. J. O. HIRSCHFELDER, C. F. CURTISS, R. B. BIRD, *Molecular theory of gases and liquids*, N. Y.-London 1954.
5. R. S. DEVOTO, Phys. Fluids, **9**, 6, 1230, 1966.
6. R. S. DEVOTO, Phys. Fluids, **10**, 2, 354, 1967.
7. L. MONCHICK, Phys. Fluids, **2**, 6, 695, 1959.

A.F. IOFFE PHYSICAL TECHNICAL INSTITUTE
USSR ACADEMY OF SCIENCES, LENINGRAD.

Received January, 12, 1973.